# Investigation of the evaporation process of liquefied hydrocarbons in front of a compressor

Sebastian Schuster[1], Dieter Brillert[1], Uwe Martens[2], Viktor Hermes[2], Friedrich-Karl Benra[*1]

ISROMAC 2017

International Symposium on Transport Phenomena and Dynamics of Rotating Machinery

Hawaii, Maui

December 16-21 2017

**Abstract**

Inlet fogging and wet compression are well known methods to lower the inlet temperature of air compressors of gas turbines and in this way lead to a more efficient compression process. Injection of water into the gas stream is another established method to reduce the compressor stage inlet temperature during the compression of crack gas. The lower inlet temperature of the compressor stage reduces its power demand and additionally, the discharge temperature remains in a suitable range. Applying the method of liquid injection, all injected droplets should be evaporated before entering the compressor impeller to avoid damage at the blades. A good knowledge about the evaporation process of injected liquid in a free stream is necessary to determine the required distance for complete evaporation of all droplets.

The aim of this paper is to provide clear statements on technical possibilities and requirements for an optimized and reliable compression process under liquid injection. The evaporation process of injected hydrocarbon droplets into a gas stream is investigated under realistic boundary conditions. Using conservation laws of mass and energy, a 1D numerical model is derived which allows the calculation of the liquid hydrocarbon evaporation in a free stream. The required fluid properties are taken from the National Institute of Standards and Technology (NIST). A comparison between the 1D model and a 3D Navier-Stokes solution for injected $CH_4$ droplets into a $CH_4$ gas stream shows good agreement regarding the decrease of the droplet diameter during the evaporation with respect to the amount of injected mass of liquid fluid and gives a good indication of the requested distance for complete evaporation. In addition, the 1D model predicts the temperature decrease of the gas during evaporation in good accordance to a 3D Navier-Stokes solver. Applying the simple 1D model, it is possible to evaluate the thermodynamic inlet parameters of a compressor for given boundary conditions quickly. In addition, the results allow a statement regarding the complete evaporation of all sizes of injected droplets at the compressor inlet and the formation of liquid films at the walls.

**Keywords**

Liquid injection, evaporation, droplet size, liquid films, required compressor power

[1]*Chair of Turbomachinery, University of Duisburg-Essen, Germany*

[2]*Siemens AG, Dresser-Rand Business, Duisburg, Germany*

*__Corresponding author__: friedrich.benra@uni-due.de

## INTRODUCTION

Injection liquid in front of a compressor is a method used to decrease the inlet temperature of the compressor by evaporation and thereby reduce the necessary power demand for the compression process. A large field of various applications is known and executed in several implementations. The most established method is water injection into the suction chamber of a heavy-duty gas turbine (HDGT) to increase power output on hot days, for example; but there are other fields of compression processes which can benefit from the advantages of liquid injection. For example, cracked gas compressors are the most important ones to be listed. All the installed machines have a huge power demand and are worth being investigated with regard to power saving due to liquid injection. In addition, the lower discharge temperature prevents the polymerization of cracked gas. In liquefied natural gas (LNG) supply chains, the costs can be considerably reduced by injecting liquid hydrocarbons into the gas stream.

Injecting water droplets in front of a gas turbine compressor has been the subject of research for several decades. So called wet compression has been applied in several power stations to augment the power output on hot days due to the decreased inlet temperature and an increased mass flow [1 - 4]. The investigation of single water droplet evaporation in an environment of ambient air at rest for low pressures and low temperatures is performed by Matz et al. [5]. Experimental results of droplet evaporation at elevated pressure and temperature levels in a moving air flow are published by Schnitzler [6] and Kefalas [7]. Based on their measurements a droplet evaporation model

introduced by Abramzon and Sirigano [8] is extended for polydisperse sprays and droplet breakup. In addition, the gas moves with a velocity close to real compressor fluid velocities and the slip between the droplet and the air flow is taken into consideration [9].

Usually, wet compression supersaturates the inlet air and water droplets remain in the flow entering the impeller of the compressor. Also, interstage injection provides a multi-phase flow of humid air and water droplets which must be processed by the compressor. This method has the advantage of continuously cooling the fluid during the compression process by evaporation of the water droplets inside the machine. Thermodynamic analyses of wet compression processes are given by Zheng et al. [10, 11] and Bianchi et al. [3]. In Deschwanden et al. [12] the interstage injection process is described for a multi-stage axial compressor. It is shown that under application of multiple water injections a drastic decrease of the fluid temperature compared to a dry compression process can be obtained.

The risks of multiple or inter-stage injections include the formation of water films at compressor walls and compressor blade damage due to droplets which hit the blades. The impact of droplets on the blades will likely produce erosion and degrade the blades. Water films can accumulate at certain positions in the machine and can subsequently produce large secondary droplets which have a high potential of destruction. In order to avoid these risks, that a droplet should be evaporated completely before it has the chance to hit a wall of a compressor component. Thus, knowledge about the evaporation process of injected liquid into a flow stream is necessary to determine the required distance for complete evaporation under the given boundary conditions.

Generally, injecting liquid in front or into a compressor gives new opportunities for high efficient compressors. Isothermal compression has multiple advantages; not only reduced required compressor power and decreased fluid temperature, but also a reduced number of compressor stages..

Injecting water into an air stream is regarded as a multi-component system because of the different compositions of liquid and gas. To investigate the evaporation process, a multi-component model must be applied. In case of injecting the same compound as a liquid into the gas stream (for example $CH_4$ into $CH_4$) a one-component evaporation model can describe the process.

The purpose of the present contribution is to provide a method which gives clear statements on the requirements for a reliable compression process under liquid injection without sucking liquid droplets into the machine. In contrast to wet compression, injected liquid hydrocarbon droplets into a gas stream are the focus of this paper. Since the liquid is the same substance as the gas, a one-component evaporation model should be applied.

In this paper, a simple 1D model which computes the evaporation of liquid $CH_4$ (Methane) droplets in gaseous $CH_4$ is presented. The evaporation of a droplet in a straight pipe is investigated under reliable boundary conditions. In addition, an exemplary compression process of a radial compressor impeller for $CH_4$ is discussed under injection of $CH_4$ droplets.

## 1. EVAPORATION MODEL

The continuum mechanical methods for heat and mass transfer are applied to a single liquid droplet in a gas environment. At the boundary surface between the droplet and the environment the heat and mass flow can be balanced using the established conservation equations. In case of a high gas temperature and a lower liquid temperature, the gas phase transfers heat to the droplet surface. From there, the heat is conveyed into the droplet. In Fig. 1 a droplet in a gas environment is depicted together with the heat and the mass transfer in case of evaporation. Assuming that both heat flows are of the same amount, at first the droplet will heat up continuously. As such, the difference of temperature gradient from the droplet surface to the droplet center becomes smaller and smaller. Hence, the heat transfer from the surface into the droplet decreases. Because of the arising imbalance of energy, a mass flow emerges from the droplets to the gas flow which levels out the energy balance. Determining the balance of the heat and mass flows the temperature at the surface of the droplet has to be known. In a one-component evaporation process the temperature of the gas environment typically is higher than the saturation temperature of the fluid and the droplet temperature is lower than it. At the droplet surface the temperature must be equal to the saturation temperature of the fluid.

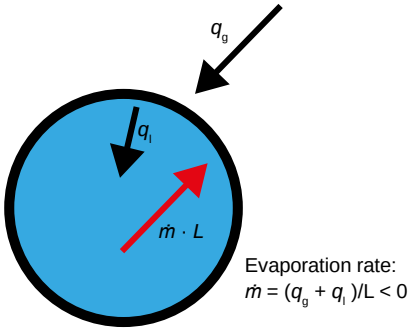


Figure 1: Evaporating droplet in a gas environment

The heat transfer can be determined with the following Nusselt-correlations:

$$q_g = \pi \cdot d_{dr} \cdot \lambda_g \cdot Nu_g \left(T_s - T_g\right) \quad (1)$$

$$q_l = \pi \cdot d_{dr} \cdot \lambda_l \cdot Nu_l \left(T_s - T_l\right) \quad (2)$$

In case of evaporation, the heat transported away from the droplet surface into the droplet is smaller than the heat transported from the gas to the surface. The difference is compensated by mass transfer using Eq. (3):

$$\frac{dm_{dr}}{dt} = \dot{m} = \frac{q_l + q_g}{L} \quad (3)$$

Empirical data are required for the Nusselt-Numbers in Eqs. (1) and (2). According to Ranz and Marshall [13, 14], the Nusselt-Number for small velocity differences between gas and droplets can be represented as $Nu_g = 2$. For the heat transfer within the droplet, a Nusselt-Number of $Nu_l = 6$ was proposed by Gerber [15].

## 2. MASS AND ENERGY CONSERVATION

In order to calculate the evaporation rate information must be available on the flow field – in particular on the gas and liquid temperatures. A 1D approach and a 3D approach are used for the investigations. The 3D approach is able to consider friction and temperature gradients orthogonal to the main flow direction.

### 2.1. One dimensional calculation

The conservation of mass along a streamline for an evaporation process can be expressed by Eq. (4):

$$\frac{d\dot{m}_g}{dt} + \dot{N}_{dr} \frac{dm_{dr}}{dt} = 0 \quad (4)$$

This expression considers the changing gas mass flow $\dot{m}_g$ and the changing droplet mass $m_{dr}$ multiplied by the number of droplets $\dot{N}_{dr}$.

The temperature of a droplet along a streamline can be calculated using Eq. (5):

$$m_{dr} c_{p,l} \frac{dT_l}{dt} = q_l + \frac{dm_{dr}}{dt} L \quad (5)$$

In an evaporation process the mixing enthalpy is constant along a streamline. At the beginning of the process the mixing enthalpy can be determined from the starting / inlet conditions (Index 0):

$$\frac{dh_m}{dx} = 0 \quad (6)$$

$$h_m = \frac{\dot{m}_{g,0} h_{g,0} + \dot{m}_{l,0} h_{l,0}}{\dot{m}_{g,0} + \dot{m}_{l,0}} = \left(1 - w_0\right) h_{g,0} + w_0 h_{l,0} \quad (7)$$

And at any downstream point the enthalpy of the gas phase can be computed as follows:

$$h_g = \frac{h_m - w \cdot \left(h_{l,ref} + c_{p,l}\left(T_l - T_{ref}\right)\right)}{\left(1 - w\right)} \quad (8)$$

With an appropriate equation of state and isobaric conditions, the gas temperature can be determined.

The number of droplets is kept constant during the complete evaporation process:

$$\dot{N}_{dr} = \frac{\dot{m}_l}{m_{dr}} \quad (9)$$

### 2.2. 3D flow calculation

The 3D flow calculations are done with an extension of ANSYS CFX. The Eulerian-Lagrangian framework is chosen to account for the conservation of mass, momentum and energy of the gas, and the liquid phase. In terms of evaporation, the main difference is that the gas total enthalpy is conserved and not the mixture enthalpy. For this approach, a source term is required in the energy equation to account for the energy transport with the evaporated mass. The convective heat transfer and the evaporated mass are calculated with the same equations presented in paragraph 1; namely Eqs. (1), (2) and (3).

## 3. FLUID PROPERTIES

The employed fluid properties for $CH_4$ are taken from NIST database [16]. In the case of evaporation in a pipe, the pressure is nearly constant along the pipe and fluid properties can be calculated with sufficient accuracy as functions of the temperature only. In order to accelerate the computation speed in the required range of temperature all fluid data are represented by polynomial descriptions as function of the temperature. Compared to the NIST data the polynomials give nearly no deviation to the reported data.

## 4. RESULTS

### 4.1 Pipe

In order to test the results for plausibility the computed results for the evaporation process of liquid $CH_4$ injected into a pipe are presented in this section and compared to each other and to the temperature after complete evaporation in an isobaric and isenthalpic process. The conveyed gas in the pipe is also $CH_4$. The velocity of the injected $CH_4$ droplets is equal to the gas velocity all the time.

#### *4.1.1 Comparison of calculation methods*

All calculations in this section are conducted under the assumption that the velocity of the droplets keeps constant along the complete evaporation distance. In addition, it is assumed that the gas volume

also stays constant during the evaporation process and thus the gas velocity is constant along the distance.

The computational fluid dynamics (CFD) simulations in this section are conducted under the assumption of no friction at the walls of the pipe in order to allow a comparison to the 1D calculations. Comparing the calculated temperature of an evaporation process of $CH_4$ in a free gas stream also consisting of $CH_4$ results of both methods are in an excellent agreement for a wide range of liquid mass flow rates (see Fig. 2). The calculated decrease in temperature due to evaporation shows an excellent agreement for both methods (see Fig. 2)

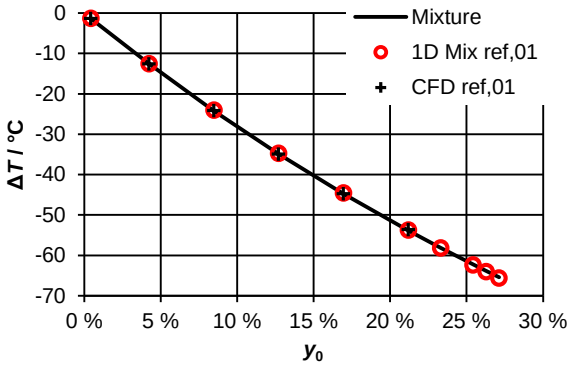


Figure 2: Decrease in gas temperature after complete evaporation of $CH_4$ droplets in a $CH_4$ gas stream

In Fig. 3 the necessary evaporation time is depicted versus the injected liquid mass (3a) and versus the droplet diameter (3b).

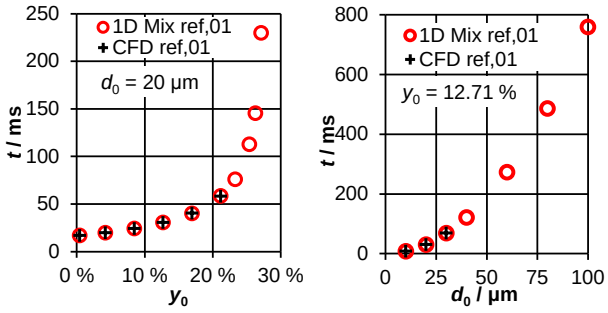


Figure 3: Evaporation time as a function of injected liquid mass (a) and as a function of droplet diameter (b)

The decrease in temperature as a function of the residence time *t* in the pipe is shown in Fig. 4 for a certain injected liquid mass and for droplets having a diameter of 20 µm. As can be seen, the temperature decreases continuously from the injection point and reaches a stable temperature after 30 ms. All droplets are evaporated at that point.

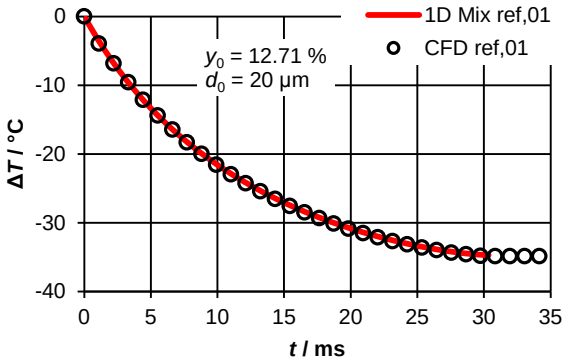


Figure 4: Temperature decrease along the pipe

### *4.1.2 Evaporation considering gas volume increase and slip between droplets and gas*

Evaporation of the liquid generates a volume of additional gas which tends to increase the gas velocity in a pipe having a constant diameter. Furthermore, the temperature of the gas decreases as another result of the evaporation. Both phenomena have an opposing effect on the gas velocity and are considered in this section. Additionally, in this chapter the CFD simulations are conducted considering friction at the pipe walls and also the slip between the droplets and the gas flow. The resistance force acting on the droplets and vice versa on the gas is determined using the Schiller-Naumann correlation [17].

Fig. 5 shows the required time[1] for complete evaporation as a function of the droplet diameter and the injected liquid mass. It is obvious that the droplet diameter should be as small as possible to achieve a short evaporation distance. In addition, the larger the injected liquid mass the longer the evaporation distance. This result proposes a clear target: small droplet diameters and a precisely adjusted liquid mass flow rate are necessary to achieve short evaporation distances.

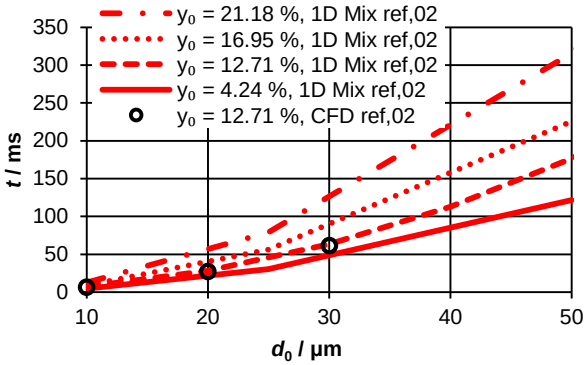


Figure 5: Evaporation time as a function of droplet diameter and injected liquid mass

The results of the 1D model and the CFD simulation are again in good accordance which means that the friction at the pipe walls and the slip between droplets and gas velocity plays a minor role. Increasing

[1] The time is calculated from the evaporation distance and the velocity at the inlet

the gas velocity at the inlet of the pipe leads to a linear extension of the evaporation distance.

### *4.1.3 Injection of a high amount of liquid*

This section of the paper investigates which consequences will arise when injecting a large amount of liquid into the gas stream. The amount (50% of mass) is much bigger than the amount which can be evaporated under the given boundary conditions. The CFD simulation shows a strong temperature decrease starting at the injection point (see Fig. 6). The temperature is much smaller than the achieved temperature under injection of 12.7% mass only (Fig. 4), but not all droplets evaporate.

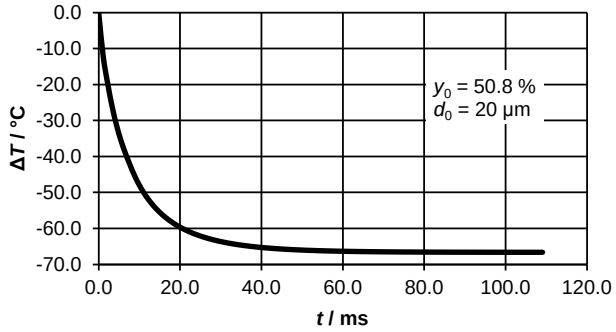


Figure 6: Trend of decrease in gas temperature at a high amount of injected liquid. Computed with CFD

The possible deposition of droplets is investigated using another 1D model. Based on the existing inlet boundary conditions, no liquid evaporation is considered for this case. This conservative assumption is the worst case and leads to the highest possible deposition rate.

The liquid is injected parallel to the gas flow which prevents droplet deposition by laminar inertia effects. Thus, only effects of diffusion and turbulent fluctuations are investigated. The deposition rate $G_{dep+}$ can be described using the non-dimensional particle relaxation time $\tau_{dr+}$ and the particle flow density $\rho_{flow}$.

$$\tau_{dr+} = \frac{1}{18}\frac{\rho_{dr}}{\rho_g}\left(\frac{d_{dr}u_\tau}{\nu_g}\right)^2 \tag{10}$$

$$G_{dep+} = \frac{G_{dep}}{\rho_{flow}u_\tau} \tag{11}$$

$$\rho_{flow} = \frac{\dot{m}_{dr}\big|_A \cdot \Delta t}{\pi \cdot r_{pipe}^2 \cdot l} = \frac{\dot{m}_{dr}\big|_A \cdot \frac{l}{u}}{\pi \cdot r_{pipe}^2 \cdot l} = \frac{\dot{m}_{dr}\big|_A}{\pi \cdot r_{pipe}^2 \cdot u} \tag{12}$$

The wall shear forces are computed according to Schlichting [18] as:

$$u_\tau = \sqrt{\tau_w / \rho_g} \tag{13}$$

$$\tau_w = \frac{\rho_g}{2}u_g^2\frac{\lambda}{4} \tag{14}$$

$$\lambda = 8\left(1.35\frac{0.41}{ln\,\mathrm{Re}}\right)^2 \quad \text{for } 2300<\mathrm{Re}<10^7 \tag{15}$$

$$Re = \frac{\rho_g u_g d_{pipe}}{\mu_g} \tag{16}$$

To determine the deposition rate experiments about particle deposition in pipes from Sehmel [19] as well as Liu and Agarwal [20] are used. These results are depicted in Fig. 7 together with the linear approximation for the three distinguished areas.

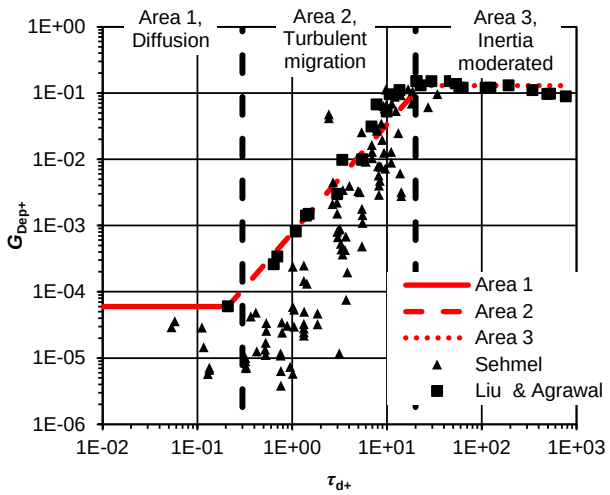


Figure 7: Measured deposition rates in pipes [19, 20]

The thickness of the developed liquid film is determined using an adapted approach from Schuster et al. [21]. In an iterative procedure, the film thickness is calculated considering a shear force between liquid and gas phase impressed from the gas phase and the velocity of the liquid film. The wall shear force of the liquid is computed under the assumption of a laminar velocity profile.

The results are depicted in Fig. 8 for very small droplets (1 µm) and for droplets of a standard size (20 µm). The figure clearly shows that the thickness of the wall film increases rapidly within the first distance after injection of the big droplets. For the very small droplets the wall film thickness increases to a thickness of only 2 µm. It is likely that the film breaks-up into rivulets having a larger thickness.

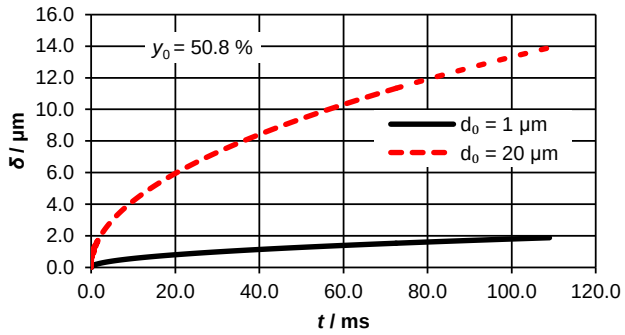


Figure 8: Thickness of liquid film at pipe wall as a function of the through-flow time

### 4.2 Compressor

Injecting liquid in front of a compressor impeller reduces the temperature increase during the change of state. The investigation of droplet evaporation in a compressor impeller can be treated almost the same as in a pipe. A major difference is that rothalpy keeps constant:

$$H_{\mathrm{rot}} = h_{\mathrm{m}} - \frac{1}{2}u^2 + \frac{1}{2}w^2 = const. \qquad (17)$$

To determine the mixing enthalpy from Eq. (17) information on the circumferential velocity *u* and on the relative velocity *w* are required. The computation of these values from velocity triangles is straightforward. The definition of velocity triangles instead of using arbitrary geometry is a comprehensible way to investigate the benefits of evaporation in the impeller. The velocity triangles are defined at the inlet and the outlet, together with a suitable change in relative flow angle between inlet and outlet. In a later step, the impeller geometry can be computed from the velocity triangles and from the gas properties; however, this is beyond the scope of this paper. For the following investigations, common assumptions are used: The flow is swirl-free at the inlet; meridional velocity is constant; flow is strictly radially-oriented at the outlet; the flow angle ($\beta$) changes linear between inlet and outlet. Therefore, all requested information about the flow are given and result in the velocity triangles depicted in Fig. 9, together with the meridional view. The shroud contour is only for illustration purposes and must be computed after determining the density along the mean line.

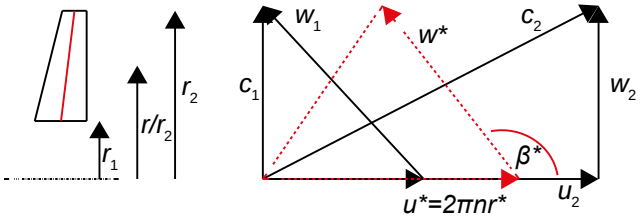


Figure 9: Meridional view with the mean streamline (red) and velocity triangles of a radial impeller as an example

As the fluid properties are a function of the temperature and the pressure, the static pressure should be known at the inlet of the impeller. With the given information, the pressure increase along a streamline can be described in an approximate manner by the following equation:

$$\int v\,dp = y = \eta \cdot \Delta h_{\mathrm{m}} \approx \frac{\Delta p}{\rho} \qquad (18)$$

For a given polytropic efficiency, which is assumed to be constant from impeller inlet to impeller outlet, the pressure can be calculated from Eq. (18) for small steps along the radius of the streamline through the impeller. In Figs. 10a and 10b, the pressure increase and temperature increase in a radial compressor impeller are depicted for a complete dry (no injection) process and for a process with injection of a small amount of liquid mass ($y$ = 5 %) and small droplets (5 µm).

It´s obvious that during the compression process the outlet pressure slightly increases when injecting liquid due to the higher density of the fluid, but a remarkable outlet temperature decrease occurs in comparison to the complete dry process. This situation provides incentive to inject liquid in front of a compressor which should evaporate during the compression process. The evaporation of the droplets in the compressor impeller allows operators to reach nearly the same pressure ratio but with a much smaller outlet temperature for the same power input.

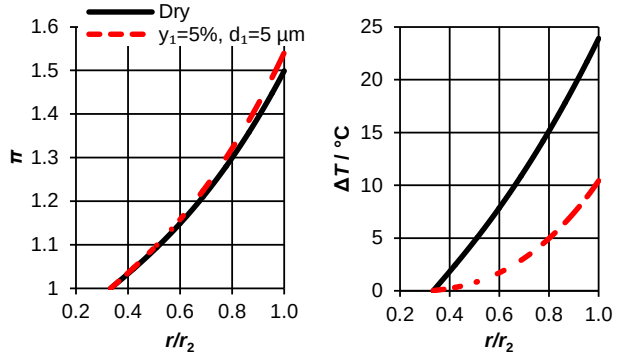


Figure 10: Course of pressure ratio and temperature increase along the radial coordinate in a radial impeller under liquid evaporation

The advantage of liquid injection becomes clearer when the geometry of the compressor impeller is adjusted in order to reach the same outlet pressure compared to the dry compression. Reducing the outlet diameter of the impeller and keeping the impeller outlet flow angle at the same magnitude ($\beta_2$ = 90°) allows to calculate the requested compressor power from the Euler equation multiplied by the overall mass flow (gas + evaporated liquid + liquid).

In Fig. 11, a comparison of the power requirement of a radial compressor for injection of different amounts of liquid is plotted versus the droplet diameter. Under the assumption of complete evaporation at the impeller outlet, the biggest power savings can be realized with the highest amount of injected liquid ($y$ = 15 %) and with the smallest droplet diameter (5 µm). This result is not surprising but clearly shows the trend: the smaller the droplets are, the greater the power savings and the more liquid can be injected.

The reduction of required compressor power approaches zero for injected liquid droplets larger than 50 µm independent of the injected amount, because as shown before in Fig. 5 the droplets will not evaporate within the available distance.

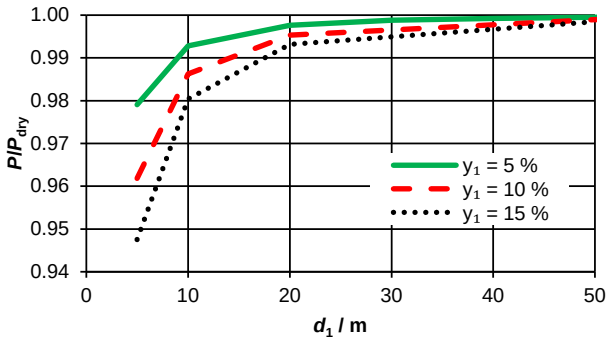


Figure: 11 Possible reduction of required compressor power due to liquid injection

## 5. CONCLUSIONS

This paper provides an insight into the injection of liquid hydrocarbons into a gas stream of the same composition. To evaluate the evaporation of the injected droplets, two different calculation methods are applied. Under the given assumptions the results of the 1D method are comparable to the results of the CFD simulations. Using the easy-to-handle 1D method which gives results in a short response time it is possible to quickly estimate the required distance for complete evaporation of the droplets. In addition, for a defined evaporation time the parameters of the applied injection nozzles can be specified in order to get droplets as small as required.

If it is indispensable to evaporate all injected droplets before they reach the impeller of the compressor, the temperature decrease of the gas and the mass flow gained are the benefits of the liquid injection. But if it´s permissble for the compressor to suck in certain size droplets, the evaporation during the compression process will be another benefit which reduces the outlet temperature of the gas and the power requirement of the compressor. Droplet diameters below 10 µm are necessary to gain a remarkable benefit of evaporation in the impeller.

The results presented in this paper show the feasibility of the technology and justify further investigation. The next steps of research should be the investigation of the impact of droplet/droplet interaction and the interaction of droplets with the surrounding walls on the evaporation process. In this context the behavior of liquid films and the generation of secondary droplets should be a focus. Another point of investigation is the definition of a droplet diameter spectrum because no available nozzles can produce a mono dispersed spray.

## ACKNOWLEDGMENTS

The authors would like to acknowledge the financial support and the permission for publication of the results for this project from Siemens AG, Dresser-Rand business, Duisburg, Germany.

## NOMENCLATURE

### Latin symbols

| | | |
|---|---|---|
| $A$ | m² | area |
| $c_p$ | kJ/kgK | specific heat capacity at constant pressure |
| $c$ | m/s | absolute velocity |
| $d$ | µm | droplet diameter |
| $G_{dep+}$ | - | deposition rate |
| $h$ | kJ/kg | specific enthalpy |
| $H_{rot}$ | kJ/kg | spec. rothalpy |
| $l$ | m | pipe length |
| $L$ | kJ/kg | latent heat |
| $m$, $\dot{m}$ | kg, kg/s | mass, mass flow |
| $\dot{N}$ | 1/s | number per time |
| $n$ | 1/s | rotational speed |
| $P$ | W | power |
| $p$ | bar | pressure |
| $\Delta p$ | bar | pressure difference |
| $q$ | W | heat flux |

| | | |
|---|---|---|
| *r* | m | radius |
| *t* | s | time |
| *T* | °C | temperature |
| *u* | m/s | velocity |
| $u_\tau$ | m/s | friction velocity |
| *v* | $m^3$/kg | spec. volume |
| *w* | m/s | relative velocity |
| *w* | - | liquid mass fraction related to the mass of mixture |
| *x* | m | axial distance |
| *y* | - / kJ/kg | liquid mass fraction related to the gas mass / specific work |

**Greek symbols**

| | | |
|---|---|---|
| *α* | W/(m²·K) | heat transfer coefficient |
| *δ* | µm | thickness |
| $\eta$ | | polytropic efficiency |
| $\lambda$ | W/(m·K)/- | heat conductivity / friction coefficient |
| $\mu$ | Pa·s | dynamic viscosity |
| $\pi$ | - | pressure ratio |
| $\rho$ | kg/m³ | density, particle flow density |
| $\tau_{dr+}$ | - | particle relaxation time |
| $\tau_W$ | | shear force |

**Indices**

| | |
|---|---|
| *0* | boundary conditions inlet |
| *1, 2* | inlet, outlet of impeller |
| *dep+* | deposition |
| *dr* | droplet |
| *g* | gas |
| *l* | liquid |
| *m* | mixing/mixture |
| *ref* | reference |
| *s* | saturation |

**Abbreviations**

| | |
|---|---|
| CFD | Computational Fluid Dynamics |
| NIST | National Institute of Standards and Technology |

**Non-dimensional numbers**

$$Nu = \frac{\alpha \cdot d}{\lambda}$$ Nusselt-Number

$$Re = \frac{u \cdot \rho \cdot l}{\mu}$$ Reynolds-Number

## REFERENCES


[1] Chaker, M. A., Meher-Homji, C. B., Mee, T., Inlet Fogging of Gas Turbine Engines – Experimental and Analytical Investigations on Impacting Pin Fog Nozzle Behavior, Proceedings of ASME Turbo Expo 2003, GT2003-38801, Atlanta, Georgia, USA

[2] Bhargava, R. K., Bianchi, M., Chaker, M., Melino, F., Peretto, A., Spina, P. R., Gas Turbine Compressor Performance Characteristics During Wet Compression – Influence of Polydisperse Spray, Proceedings of ASME Turbo Expo 2009, GT2009-59920, Orlando, USA

[3] Bianchi, M., Melino, F., Peretto, A., Spina, P. R., Ingistov, S., Influence of Water Droplet Size and Temperature on Wet Compression, Proceedings of ASME Turbo Expo 2007, GT2007- 27458, Montreal, Canada

[4] Bianchi, M., Chaker, M., de Pascale, A., Peretto, A., Spina, P. R., CFD Simulation of Water Injection in GT Inlet Duct Using Spray Experimentally Tuned Data: Nozzle Spray Simulation Model and Results for an Application to a Heavy Duty Gas Turbine, Proceedings of ASME Turbo Expo 2007, GT2007-27361, Montreal, Canada

[5] Matz, C., Kappis, W., Cataldi, G., Mundinger, G., Bischoff, S., Helland, E., Ripken, M., Prediction of Evaporative Effects Within the Blading of an Industrial Axial Compressor, Proceedings of ASME Turbo Expo 2008, GT2008-50166, Berlin Germany

[6] Schnitzler, J. P., Feng, J., Benra, F.-K., Dohmen, H. J., Werner, K., Test Rig Design for Investigation of Water Droplet Evaporation at High Pressure and Temperature Levels, Proceedings of the 14th International Symposium on Transport Phenomena and Dynamics of Rotating Machinery (ISROMAC-14) 2012, Honolulu, HI, USA

[7] Kefalas, A., Barabas, B., Schnitzler, J., Benra, F.-K., Dohmen, H. J., Water Droplet Evaporation at High Pressure and Temperature Levels – Part 1: Experimental investigations of the spray pattern in dependence on parameter variation, Proceedings of the 9th International Conference on Heat Transfer, Fluid Mechanics and Thermodynamics (HEFAT 2012), Malta

[8] Abramzon, B., Sirigano, W. A., Droplet vaporization model for spray combustion calculations, International Journal of Heat and Mass Transfer, Vol. 32, 1989

[9] Barabas, B., Kefalas, A., Schnitzler, J., Rossetti, A., Benra, F.-K., Dohmen, H. J., Water droplet evaporation at High gas pressure and temperature levels – Comparison of experimental results with a one-dimensional simulation, Journal of Computational Thermal Sciences, 5 (3), 2013

[10] Zheng, Q., Sun, Y., Li, S, Wang, Y., Thermodynamic Analyses of Wet Compression Process in the Compressor of Gas Turbine, ASME Journal of Turbomachinery, 125 (3), 2003

[11] Zheng, Q., Li, M., Sun, Y., Thermodynamic Performance of Wet Compression and Regenerative (WCR) Gas Turbine, Proceedings of ASME Turbo Expo 2003, GT2003-820, Atlanta, Georgia, USA

[12] v. Deschwanden, I., Droplet evaporation in the context of interstage injection, Proceedings of the 16th International Symposium on Transport Phenomena and Dynamics of Rotating Machinery (ISROMAC-16) 2016, Honolulu, HI, USA

[13] Ranz, W. E., Marshall, W. R., Evaporation from drops Part 1. Chemical Engineering Progress, 48, Vol. 3, 1952

[14] Ranz, W. E., Marshall, W. R., Evaporation from drops Part 2. Chemical Engineering Progress, 48, Vol. 4, 1952

[15] Gerber, A. G., Inhomogeneous Multifluid Model for Prediction of Nonequilibrium Phase Transition and Droplet Dynamics, J. Fluids Eng., 130(3), doi:10.1115/1.2844580 , 2008

[16] Lemmon, E. W., McLinden, M. O., Friend, D. G., Thermophysical Properties of Fluid Systems, NIST Chemistry WebBook, NIST Standard Reference Database Number 69, Eds. P.J. Linstrom and W.G. Mallard, National Institute of Standards and Technology, Gaithersburg MD, 20899, doi:10.18434/T4D303

[17] Schiller, L., Naumann, A., Über die grundlegende Berechnung bei der Schwerkraftaufbereitung, Zeitschrift des Vereins Deutscher Ingenieure, 1933

[18] Schlichting, H., Grenzschichttheorie, Berlin Heidelberg New York, Springer-Verlag, 2006, 978-3-540-32985-5

[19] Sehmel, G., Aerosol deposition from turbulent airstream in vertical conduits, AEC Research & Development Report, BNWL-578, 1968

[20] Liu, B. Y. H., Agarwal, J. K., Experimental observation of aerosol deposition in turbulent flow, Aerosol Science, Pergamon Press, Vol. 5, 1974

[21] Schuster, S., et al., Sensitivity analysis of condensation model constant on calculated liquid film motion in radial turbines, Proceedings of ASME Turbo Expo 2014, GT2014-25652, Düsseldorf, Germany